

Flux Noise and Fluctuation Conductivity in Unfrustrated Josephson Junction Arrays

Ing-Jye Hwang*, Seungoh Ryu and D. Stroud

Department of Physics, The Ohio State University, Columbus, Ohio 43210

(March 23, 2022)

Abstract

We study the flux noise $S_{\Phi}(\omega)$ and finite frequency conductivity $\sigma_1(\omega)$ in two dimensional unfrustrated Josephson junction arrays (JJA's), by numerically solving the equations of the coupled overdamped resistively-shunted-junction model with Langevin noise. We find that $S_{\Phi}(\omega) \propto \omega^{-3/2}$ at high frequencies ω and flattens at low ω , indicative of vortex diffusion, while $\sigma_1 \propto \omega^{-2}$ at sufficiently high ω . Both quantities show clear evidence of critical slowing down and possibly scaling behavior near the Kosterlitz-Thouless-Berezinskii (KTB) transition. The critical slowing down of S_{Φ} , but not its frequency dependence, is in agreement with recent experiments on Josephson junction arrays.

PACS numbers: 74.50.+r, 74.40.+k, 64.60.Fr

Josephson junction arrays (JJA's) and thin-film superconductors are excellent model systems for studying vortex dynamics. At zero magnetic field, such systems are believed to undergo a Kosterlitz-Thouless-Berezinskii^{1,2} (KTB) transition at a temperature T_{KTB} . At temperatures below T_{KTB} the vortices and anti-vortices are bound into pairs, whereas above T_{KTB} these pairs start to unbind into unpaired vortices. Such a phase transition is expected to affect a variety of transport properties of such systems.³ Measurements of both the IV characteristics and the inverse kinetic inductance consistent with the occurrence of a KTB transition have been reported in both thin superconducting films⁴ and superconducting arrays.⁵

A particularly sensitive probe for such vortex dynamics is the study of flux noise. Conventional transport properties such as the IV characteristics, while sensitive to vortex dynamics, are typically nonequilibrium measurements, requiring the application of an external current. By contrast, magnetic flux noise is typically measured at equilibrium, by placing a superconducting quantum interference device (SQUID) over a portion of the array or film. Such a measurement is sensitive to equilibrium fluctuations in the local vortex number of vortices within that area.

A number of groups have studied flux noise in superconductors. Several measurements have been carried out in high temperature superconducting films, including $\text{Bi}_2\text{Sr}_2\text{CaCu}_2\text{O}_{8+\delta}$ ⁶ and $\text{YBa}_2\text{Cu}_3\text{O}_{6.95}$.⁷ Recently, Shaw *et al.*⁸ have done noise experiments on overdamped JJA's consisting of superconducting Nb islands in a Cu film, greatly extending some earlier measurements by Lerch *et al.*⁹ These experiments yield a range of behavior for the spectral function $S_\Phi(\omega)$ of the flux noise, that is, the frequency Fourier transform of the flux-flux correlation function. For example, $\text{YBa}_2\text{Cu}_3\text{O}_{6.95}$ ⁷ and JJA's⁸ are found to have $S_\Phi(\omega) \propto \omega^{-1}$ at "high" frequencies ("high," in this context, meaning greater than about 10-1000 Hz), while in $\text{Bi}_2\text{Sr}_2\text{CaCu}_2\text{O}_{8+\delta}$ ⁶ $S_\Phi(\omega) \propto \omega^{-3/2}$ at similar frequencies.

There have also been several theoretical studies of flux noise in such systems. Houlik *et al.*¹⁰ discussed the behavior of flux noise from a Coulomb gas analogy, and calculated $S_\Phi(\omega)$ from a time-dependent Ginzburg-Landau (TDGL) model. At high frequencies, they found

$S_{\Phi}(\omega) \propto \omega^{-2}$. Gronbech-Jensen *et al.*¹¹ studied a JJA with a static magnetic field of $1/2$ flux quantum per plaquette, using the so-called resistively shunted junction (RSJ) model including self-capacitance. Their primary interest, however, was to find the voltage noise at finite external currents, with disorder in the islands' positions, rather than the flux noise itself. Recently, Wagenblast and Fazio¹² have studied the flux noise and scaling behavior using an XY -model with an assumed local damping for the phases. The local damping term corresponds to ohmic resistance shunts coupling each superconducting grain to the ground. The resulting flux noise was found to be white for low frequencies, varied as ω^{-2} at high frequencies, and as ω^{-1} at intermediate frequencies. Very recently, Tiesinga *et al.*¹³ have used both the coupled RSJ model and a TDGL model to study flux noise numerically over a relatively limited frequency range. They concluded that their TDGL results were closer to the experiment of Shaw *et al.*⁸ than were the RSJ predictions.

In this paper, we carry out extensive calculations of flux noise in an array of coupled overdamped Josephson junctions, using Langevin noise to simulate the effects of temperature. Our model is similar to that of Tiesinga *et al.*¹³, but we study the real part of the frequency-dependent fluctuation conductivity $\sigma_1(\omega)$ in addition to the vortex noise, and we calculate both over a considerably wider frequency regime. Our results for the flux noise show a clear signature of vortex diffusion above T_{KTB} , i. e., $S_{\Phi}(\omega) \propto \omega^{-3/2}$ above a cut-off frequency $\omega_v(T)$ which approaches zero near T_{KTB} . $\sigma_1(\omega)$ is found also to have a characteristic frequency $\omega_{\sigma}(T)$ which approaches zero on either side of T_{KTB} .

The details of the RSJ model can be found in the literature.¹⁴ The current through a junction between two superconducting islands i and j is assumed to consist of three contributions in parallel: a normal current $I_{R;ij} = V_{ij}/R_{ij}$ through a resistance R_{ij} ; a Josephson current $I_{S;ij} = I_{c;ij} \sin(\theta_{ij})$; and a thermal noise current $I_{L;ij}$. Here $I_{c;ij}$ is the critical current, $\theta_{ij} = \theta_i - \theta_j$ is the phase difference across the junction, and $V_{ij} \equiv V_i - V_j$ is the voltage between islands i and j . The use of Kirchhoff's law for current conservation and of the Josephson relation $V_{ij} = (\hbar/2e)(d\theta_{ij}/dt)$ leads to a set of coupled first-order nonlinear differential equations. We solve these coupled equations numerically by a standard algorithm

for square lattices of several sizes, as discussed, for example, by Chung *et al.*¹⁴ We assume no external current, and use periodic boundary conditions for an $N \times N$ square lattice of size $N_s = N \times N$ with no disorder, i. e., $I_{c;ij} = I_c$ and $R_{ij} = R$ for all i, j , and no external magnetic field. The time iteration is accomplished using a second-order Runge-Kutta procedure with time intervals of order $dt = 0.01\tau_0$, where $\tau_0 = \hbar/(2eRI_c)$ is the characteristic time of the problem. By means of the assumed Langevin dynamics, we can calculate not only time-dependent quantities, but also various equilibrium quantities¹⁵, computed as time averages. In the following, our results are presented in the “natural units” of the problem. Thus, the natural unit of time is τ_0 , and of frequency, $\omega_0 = 1/\tau_0$. Energy and temperature are given in units of $\hbar I_c/(2e)$.

Many of the physical observables of interest are spectral functions, that is, the Fourier transforms of various time correlation functions. For an observable $O(t)$, the spectral function is defined as

$$S_O(\omega) = \frac{1}{N_s} \times \lim_{\Theta \rightarrow \infty} \frac{1}{\Theta} \left| \int_{-\Theta/2}^{\Theta/2} O(t) e^{-i\omega t} dt \right|^2. \quad (1)$$

With this definition, $S_O(\omega)$ has dimensions $[O^2 \cdot t]$, where t denotes time.

Fig. 1 shows the time-averaged mean-square vortex density $\Delta n_z = (1/N_s) \sum_{\mathbf{r}} n_z^2(\mathbf{r})$ for zero magnetic field. Here $n_z(\mathbf{r}) = 0$ or ± 1 denotes the number of vortices in the \mathbf{r}^{th} plaquette, as conventionally defined.¹⁶ Δn_z becomes nonzero near T_{KTB} , where the vortex-antivortex pairs begin to unbind. T_{KTB} , as estimated from the vanishing of Δn_z , is close to the accepted value of $0.9-0.95\hbar I_c/(2ek_B)$ for an infinite lattice.¹⁷

Another quantity of interest is the helicity modulus γ ,¹⁸ which measures stiffness against long-wavelength twists of θ , and is proportional to the superfluid density. Fig. 2 shows γ and the integral of the fluctuation conductivity, $\gamma_2 = (1/\pi) \int_{-\infty}^{\infty} \sigma_1(\omega) d\omega$, where $\sigma_1 = \text{Re}\sigma$. Both are calculated using standard expressions,¹⁹ but from a time-average of the RSJ solutions. γ_2 shows a characteristic peak near T_{KTB} . The expected universal jump in γ at T_{KTB} is somewhat broadened in our calculations, probably by finite-size effects.

Fig. 3(a) shows $\sigma_1(\omega)$ itself, as calculated directly from the fluctuation-dissipation

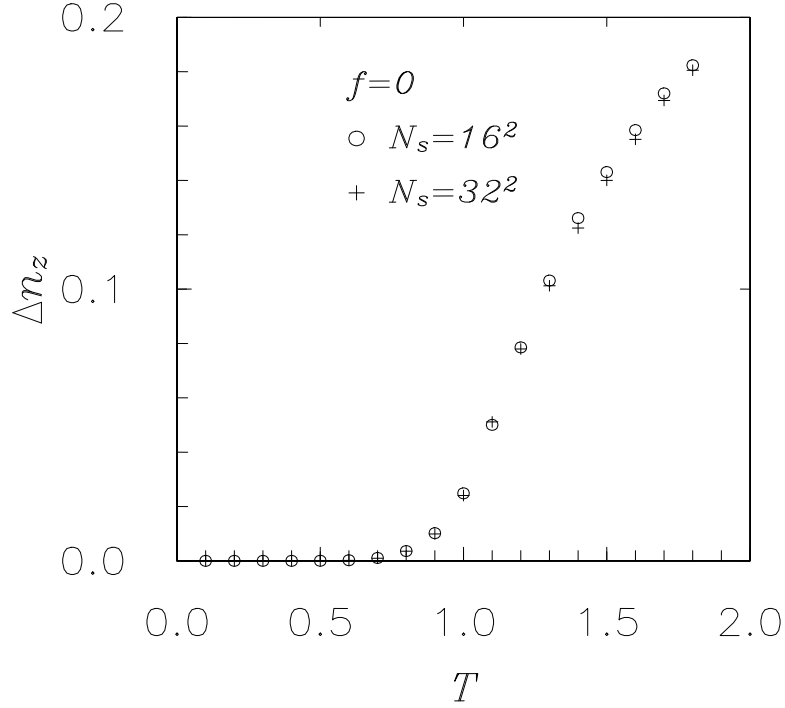


FIG. 1. Time-averaged mean-square vortex density Δn_z for the overdamped array at zero magnetic field, plotted as a function of temperature T for two different array sizes.

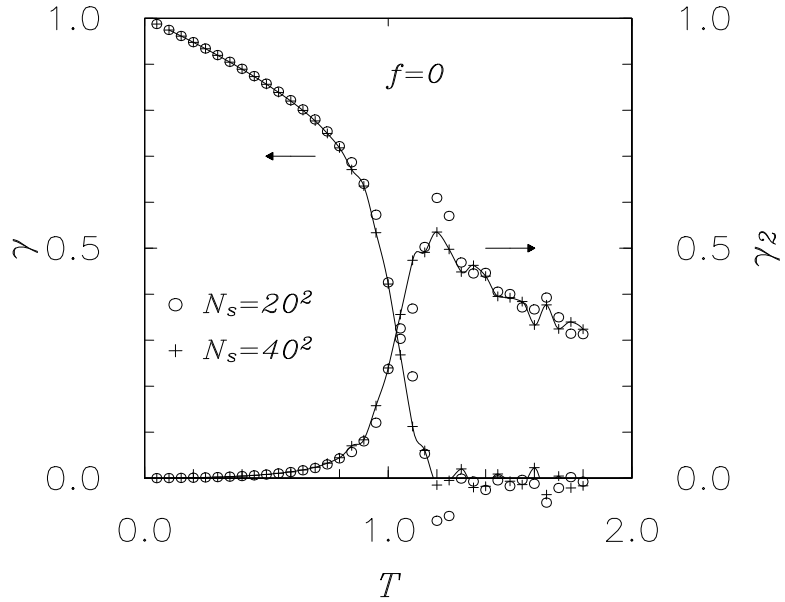


FIG. 2. Helicity modulus γ and integrated fluctuation conductivity γ_2 for an overdamped array at zero magnetic field and two different array sizes, as calculated from time-averaged solutions to RSJ equations with Langevin noise.

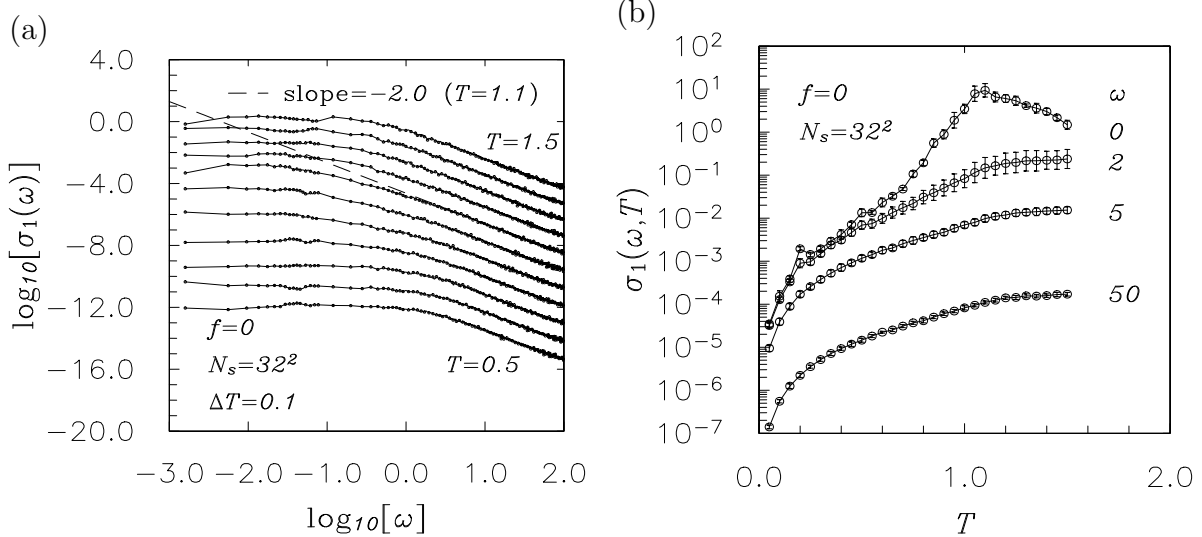


FIG. 3. Fluctuation conductivity $\sigma_1(\omega)$ (eq. 2), plotted (a) versus frequency ω for several temperatures T , and (b) versus temperature at several ω . All quantities are plotted in natural units. The curves in (a) are vertically displaced; the dashed line has slope -2 .

theorem²⁰ for several different temperatures. In the classical limit ($\hbar\omega \ll k_B T$) for this isotropic system, this theorem gives

$$\sigma_1(\omega) = \frac{1}{N_s k_B T} \sum_{\mathbf{r}, \mathbf{r}'} \int_0^\infty dt \cos(\omega t) \langle J_x(\mathbf{r}, t) J_x(\mathbf{r}', 0) \rangle, \quad (2)$$

where $J_x = \sum_{\langle ij \rangle} I_c \sin(\theta_i - \theta_j)$ is the x -component of the supercurrent. For a fixed temperature, $\sigma_1(\omega)$ flattens at low frequency and falls off at high frequencies approximately as $1/\omega^2$. The slight upward convexity at high frequency here (and for the noise calculation below) is an artifact of the fast Fourier transform used to evaluate these quantities. Fig. 3(b) shows $\sigma_1(\omega, T)$ at several fixed ω 's. At the lowest frequency (nominally $\omega = 0$, but actually an average over several $\omega < 0.08$), there is a strong peak at $T \approx T_{KTB}$ (somewhat masked by the log-log plot). For the other frequencies (all greater than ω_0), no peak is discernible near T_{KTB} , indicating that the influence of the transition is suppressed at such high frequencies. By comparing these results with those of Fig. 2, we see that the peak in γ_2 is dominated by the *low frequency* regime of $\sigma_1(\omega)$, i. e., $\omega < \omega_0$.

Next, we turn to the flux noise $S_\Phi(\omega)$. Rather than calculate this quantity, we instead calculate the somewhat simpler *vortex number noise*, $S_v(\omega)$, which should behave similarly

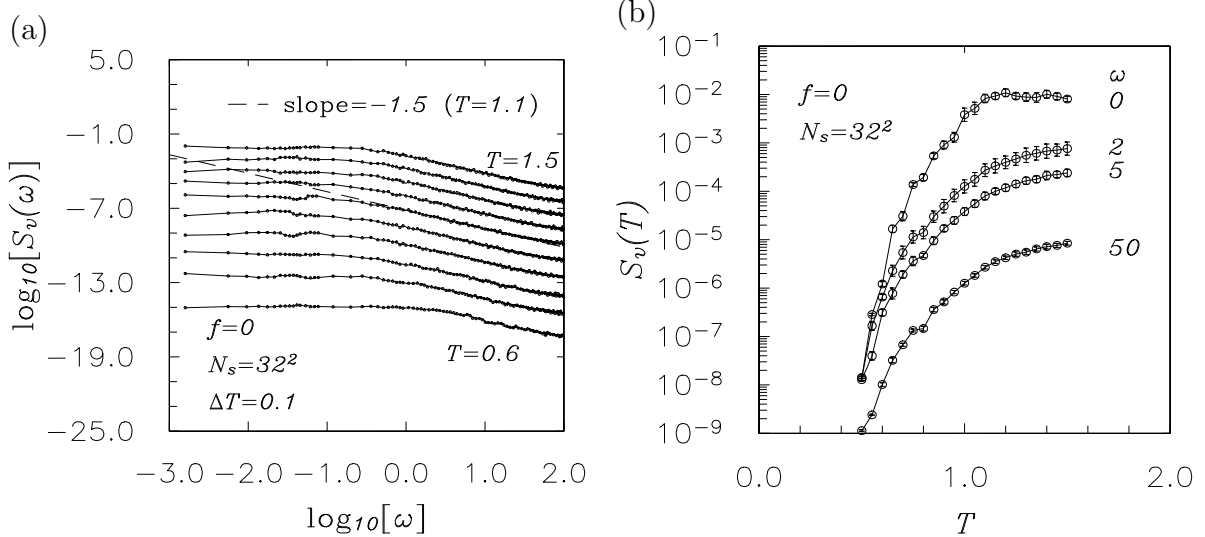


FIG. 4. Same as Fig. 3, but for $S_v(\omega)$. Dashed line has slope -1.5 .

in most cases.⁸ $S_v(\omega)$ is the noise associated with $N_v = \sum_{\mathbf{r}} n_z(\mathbf{r})$, the vortex number enclosed in the area \mathcal{A} spanned by the SQUID used to detect the flux noise. With periodic boundary conditions, N_v would be identically zero if \mathcal{A} were the entire array area. For a smaller \mathcal{A} , N_v fluctuates in time, giving rise to vortex noise. Our results are shown in Fig. 4 for a square area $\mathcal{A} \equiv \ell^2$ equal to 1/4 of the array area. Fig. 4(a) shows our results for different temperatures as a function of frequency; (b), for different frequencies as a function of T . At low frequencies, S_v becomes roughly frequency-independent, but at high frequencies $S_v(\omega) \sim \omega^{-3/2}$, a dependence which is known to characterize *diffusive behavior*.²¹ The spectral function thus clearly shows the characteristic signature of *vortex diffusion* at temperatures above T_{KTB} .

Fig. 4(a) also suggests the same critical slowing down seen in the conductivity plots. That is, the $S_v(\omega)$ plots flatten out at a temperature-dependent crossover frequency $\omega_v(T)$ [inset of Fig. 5(a)] which vanishes as $T \rightarrow T_{KTB}$ from either side. Such behavior suggests that the effective vortex diffusion coefficient $D \rightarrow 0$ as $T \rightarrow T_{KTB}$. This follows from the approximate relation²¹ $D \approx \ell^2 \omega_v$ which connects the D to the vortex noise spectrum in a fixed area ℓ^2 .

We now discuss more quantitatively the apparent critical slowing down seen in both our

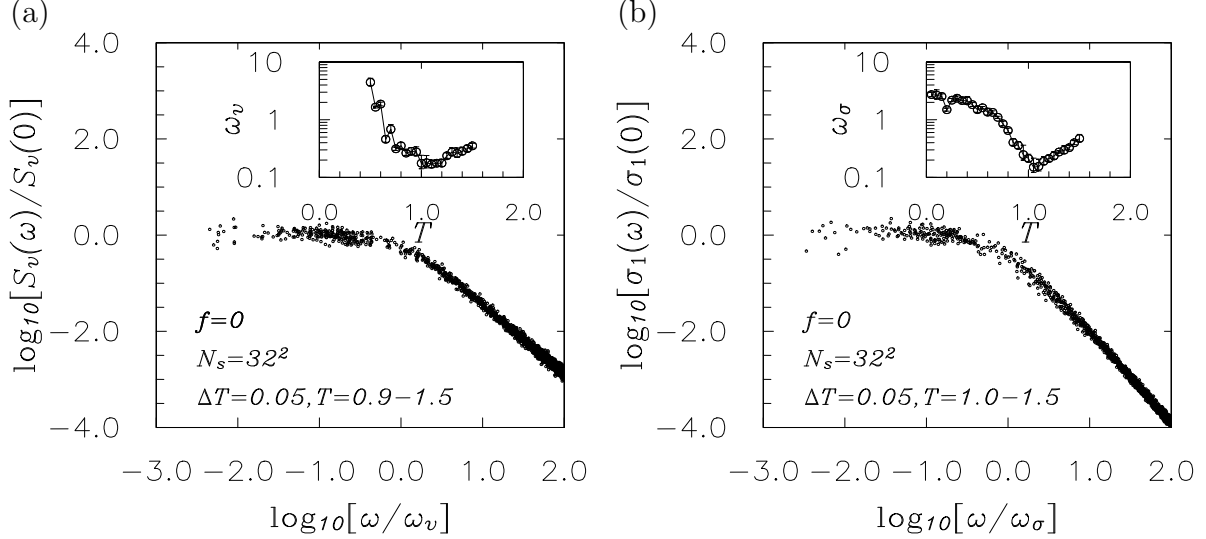


FIG. 5. (a) $S_v(\omega, T)/S_v(0, T)$ plotted against ω/ω_v , where $\omega_v(T)$ is a crossover frequency extracted from the data at each temperature and plotted in the inset. (b). $\sigma_1(\omega, T)/\sigma_1(0, T)$ plotted against ω/ω_σ , where $\omega_\sigma(T)$ is plotted in the inset.

flux noise and conductivity calculations. In the former case, Shaw *et al.*⁸ have suggested a scaling form for $S_\Phi(\omega)$ which may be written

$$\omega S_\Phi(\omega) = F\left(\frac{\omega}{\omega_\xi}\right), \quad (3)$$

where ξ is the divergent correlation length characterizing the phase transition, and F is an appropriate scaling function (we ignore any dependence on other possible scaling variables such as l/ξ). The frequency ω_ξ is expected to vary as ξ^{-z} , where z (≈ 2 experimentally⁸) is a dynamical critical exponent. A simple scaling function which appears consistent with our calculations for $S_v(\omega)$ is

$$F(x) = \frac{x}{(1+x)^{3/2}}. \quad (4)$$

As a partial test of this form, we plot in Fig. 5(a) the ratio $S_v(\omega)/S_v(0)$ against ω/ω_v , where ω_v is a crossover frequency used as a fitting parameter to the numerical data. Clearly, all the plots fall atop one another, consistent with the scaling hypothesis, and are in good agreement with the form (4), which gives the diffusive form $S_v(\omega) \propto \omega^{-3/2}$ at high frequencies. The crossover frequency ω_v [inset of Fig. 5(a)] appears to go to zero near T_{KTB} as required by

the scaling form, but our data are not adequate to test the expectation⁸ $\omega_v = \omega_\xi \propto \xi^{-2}$ with $\xi \propto \exp\left[b\sqrt{T_{BKT}/(T - T_{BKT})}\right]$. In short, our numerical results for S_v at $T > T_{KTB}$ are consistent with diffusive vortex motion in the RSJ model, and a diffusion coefficient which vanishes continuously as $T \rightarrow T_{KTB}$.

The fluctuation conductivity $\sigma_1(\omega)$ exhibits similar critical behavior, since it has the form of a Drude peak whose width goes continuously to zero as $T \rightarrow T_{KTB}$. We may anticipate a scaling form $\sigma_1(\omega) = \sigma_0/(\omega^2 + \omega_\sigma^2)$, where σ_0 has critical behavior at T_{KTB} ; this form correctly gives the calculated $1/\omega^2$ high-frequency behavior. As a partial test of this hypothesis, we have plotted in Fig. 5(b), the ratio $\sigma_1(\omega, T)/\sigma_1(0, T)$ versus ω/ω_σ for several temperatures, again using ω_σ as a fitting parameter for each temperature [inset of Fig. 5(b)]. The calculated $\sigma_1(\omega, T)$ all fall on the same universal curve both above and below T_{KTB} (for clarity, we have plotted only the temperatures above T_{KTB}). Moreover, the crossover frequencies ω_σ , like ω_v , vanish smoothly as $T \rightarrow T_{KTB}$ from either side, though again our numerical data is inadequate to confirm the functional form $\omega_\sigma \propto \xi^{-z}$ with $z \approx 2$.

Our results differ from the $1/\omega$ behavior seen experimentally for $S_\Phi(\omega)$ in overdamped Josephson arrays⁸ over several decades of frequency, although we do see indications of similar scaling behavior. Measurements on $\text{YBa}_2\text{Cu}_3\text{O}_{6.95}$ ⁷ show a similar $1/\omega$ frequency regime, but as noted earlier, studies of very thin films of $\text{Bi}_2\text{Sr}_2\text{CaCu}_2\text{O}_{8+\delta}$ ⁶ also show a $1/\omega^{3/2}$ behavior in the same (100 Hz-10KHz) frequency regime, which is also interpreted as evidence for vortex diffusion. Our results show clear evidence of such diffusive behavior in a numerical model for the dynamics of a Josephson array; the diffusing objects in our calculations, as presumably in the $\text{Bi}_2\text{Sr}_2\text{CaCu}_2\text{O}_{8+\delta}$ films, are the thermally excited vortices and antivortices. The frequencies where we find diffusive behavior appear, however, to lie well above the diffusive regime in $\text{Bi}_2\text{Sr}_2\text{CaCu}_2\text{O}_{8+\delta}$.⁶

It remains unclear why our calculations do not show a clear $1/\omega$ regime, as seen in some experiments and reported in calculations using a local damping model.¹³ One possibility is simply that we have not probed the noise spectrum to sufficiently low frequencies, or, possibly, in a sufficiently large area. In the experiments, the $1/\omega$ regime occurs in the

KHz regime, and certainly well below MHz. By contrast, our calculations do not probe frequencies much below about $0.01\omega_0 = 0.01 \ 2eRI_c/\hbar$. For typical array parameters, ω_0 may be in the range of MHz or higher, suggesting that it could be quite difficult to approach the $1/\omega$ regime in such numerical calculations.

In conclusion, we have calculated both the vortex number noise $S_v(\omega)$ and the frequency-dependent conductivity $\sigma_1(\omega)$ in an overdamped Josephson-junction array near the Kosterlitz-Thouless transition. The former exhibits a $\omega^{-3/2}$ behavior, characteristic of vortex diffusion, at high frequencies, and is flat at low frequencies. The latter has a Drude peak and a $1/\omega^2$ frequency dependence at high frequencies. Both quantities show clear evidence of critical slowing down (i. e., a vortex diffusion coefficient which goes to zero near T_{KTB}) and possible scaling behavior near the Kosterlitz-Thouless-Berezinskii transition, in agreement with experiment; but clear evidence of a $1/\omega$ regime for the vortex number noise is lacking.

This work was supported by NSF Grant DMR94-02131 and DOE Grant DE-FG02-90ER45427 through the Midwest Superconductivity Consortium. Calculations were carried out using the SP2 at the Ohio Supercomputer Center.

REFERENCES

* E-mail address: hwang@pacific.mps.ohio-state.edu.

¹ J. M. Kosterlitz and D. J. Thouless, *J. Phys. C* **6**, 1181 (1973).

² V. L. Berezinskii, *Zh. Eksp. Teor. Fiz.* **59**, 207 (1970) [*Sov. Phys. JETP* **32**, 493 (1971)].

³ V. Ambegaokar *et al.*, *Phys. Rev. B* **21**, 1806 (1980); S. Doniach and B. A. Huberman, *Phys. Rev. Lett.* **42**, 1169 (1979); P. Minnhagen, *Rev. Mod. Phys.* **59**, 1001 (1987).

⁴ M. R. Beasley *et al.*, *Phys. Rev. Lett.* **42**, 1165 (1979); A. F. Hebard and A. T. Fiory, *Phys. Rev. Lett.* **44**, 291 (1980).

⁵ D. J. Resnick *et al.*, *Phys. Rev. Lett.* **47**, 1542 (1981); D. W. Abraham *et al.*, *Phys. Rev. B* **26**, 5268 (1982); R. F. Voss and R. A. Webb, *Phys. Rev. B* **25**, 3446 (1982).

⁶ C. T. Rogers *et al.*, *Phys. Rev. Lett.* **69**, 160 (1992).

⁷ M. J. Ferrari *et al.*, *Phys. Rev. Lett.* **67**, 1346 (1991).

⁸ T. J. Shaw *et al.*, *Phys. Rev. Lett.* **76**, 2551 (1996).

⁹ Ph. Lerch *et al.*, *Helv. Phys. Acta.* **65**, 389 (1992).

¹⁰ J. Houlrik *et al.*, *Phys. Rev. B* **50**, 3593 (1994).

¹¹ N. Grønbech-Jensen *et al.* *Phys. Rev. B* **46**, 11149 (1992).

¹² K.-H. Wagenblast and R. Fazio, to be published.

¹³ P. H. E. Tiesinga *et al.*, *Phys. Rev. Lett.* **78**, 519 (1997).

¹⁴ See, e.g., S. R. Shenoy, *J. Phys. C* **18**, 5163 (1985); K. K. Mon and S. Teitel, *Phys. Rev. Lett.* **62**, 673 (1989); J. S. Chung *et al.*, *Phys. Rev. B* **40**, 6570 (1989); D. Domínguez and J. V. José, *Int. J. Mod. Phys. B* **8**, 3749 (1994).

¹⁵ See, e.g., G. Parisi, *Statistical Field Theory* (Addison-Wesley, New York, 1988), Ch. 19.

¹⁶ I.-J. Hwang and D. Stroud, Phys. Rev. B **54**, 14978 (1996).

¹⁷ S. Teitel and C. Japaprakash, Phys. Rev. B **27**, 598 (1983).

¹⁸ M. E. Fisher, M. N. Barber, and D. Jasnow, Phys. Rev. A **8**, 1111 (1973).

¹⁹ C. Ebner and D. Stroud, Phys. Rev. B **28**, 5053 (1983).

²⁰ See, e.g., L. D. Landau and E. M. Lifshitz, *Statistical Physics: Part I* (Pergamon Press, 1980), Ch. 12.

²¹ R. F. Voss and J. Clarke, Phys. Rev. B **13**, 556 (1976).